Journal of Materials Chemistry B

Accepted Manuscript

ROYAL SOCIETY OF CHEMISTRY

www.rsc.org/materialsB

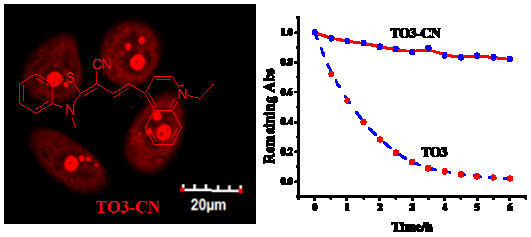

TO3-CN is a bright red fluorescent cyanine dye for live-cell nucleic acid imaging, with high photostability and large stokes shift.

Cite this: DOI: 10.1039/c0xx00000x

www.rsc.org/xxxxxx

ARTICLE TYPE

A Bright Red Fluorescent Cyanine Dye for Live-Cell Nucleic Acid Imaging, with High Photostability and Large Stokes Shift

Si Zhang, [a] Jiangli Fan, *[a] Zhiyong Li, [a] Naijia Hao, [a] Jianfan Cao, [a] Tong Wu, [a] Jingyun Wang, *[b] and Xiaojun Peng [a]

Received (in XXX, XXX) Xth XXXXXXXXX 20XX, Accepted Xth XXXXXXXXX 20XX
DOI: 10.1039/b000000x

Many probes for nucleic acids are available, but few of them satisfy in multiple criteria, particularly high photostability to endure laser scanning. We report a cyanine dye **TO3-CN** for the first time by introducing a CN group to trimethine chain of the classical red emitting TO-3 dyes to improve its photostability, as well as its spectral properties and interaction with nucleic acids. **TO3-CN** shows excellent light fastness and large fluorescence Stokes shift (more than 40 nm). Because of its sensitive fluorescence response to nucleic acids with a large fluorescence quantum yield (more than 0.7) and low cytotoxicity, this dye may be a potential candidate for nucleic acid detection *in vitro* and intracellular fluorescence imaging.

Introduction

Nucleic acids which include DNA (deoxyribonucleic acid) and RNA (ribonucleic acid), as a kind of biological macromolecule, function in encoding, transmitting and expressing genetic information, thus play a very important role in biosystems. Therefore, understanding of the organization and structure of nucleic acid *in vivo* is of great importance.

Nucleic acid-staining fluorophores have been extensively used in biological research and medical diagnosis, including cellular imaging and DNA quantification.[1-11] Although many such probes are available, only a few of them such as Hoechst and DRAQ5 are suitable for live-cell imaging. Hoechst is the most commonly used probe, but it must be excited by UV illumination, which is known to damage cellular DNA.[12, 13] DRAQ5 emits fluorescence in the deep-red region but shows high chemical cytotoxicity.[14-17] SYTO, another widely commercially available class of nucleic acid stains, do provide cell-permeable dyes excitable by visible and near-infrared radiation[18] but suffer from low photostability similar to the case with many cyanines, and moreover are of undisclosed chemical structures. In addition, the difference between emission and excitation energies (i.e., the Stokes shift) is small (typically less than 30 nm), which may lead to unwanted background signal ascribed to the autofluorescence of endogenous fluorophores.[10, 19-22] Therefore, fluorescent dyes that satisfy the multiple criteria of long-wavelength excitation/emission, high nucleic acids selectivity, excellent photostability, large Stokes shift, low cytotoxicity and live-cell permeability must be developed.[1, 23]

We have recently reported a TO-3 analogue DEAB-TO-3, as a red fluorescent live-cell-permeant DNA minor groove binder, which is a promising candidate for highly sensitive DNA detection *in vitro*, and nucleus-specific imaging and DNA quantification *in vivo*.[24] However, it also suffers from relatively low photostability owing to the fact that its trimethine-chain is longer than that of green emitting TO-1 dyes. To improve the photostability of cyanine dyes, many methods have been proposed, including the introduction of CN, F, and cyclodextrin that decrease the electron density of polymethine chains, and as a result reduce the reactivity of the dyes with singlet oxygen.[25-28] In particular, Armitage et al. reported a highly photostable green emitting dye called α-CN-TO with an strong electron withdrawing cyano group in the central methane of green emitting TO-1 to use in a protein-based fluoromodule.[28]

Herein, we report for the first time a bright red fluorescent cyanine dye, **TO3-CN**, by adding a strong electron-withdrawing CN group to the trimethine chain of the classical red emitting TO-3 dyes to improve the photostability of these dyes, as well as its spectral property and interactions with nucleic acids. Furthermore, as the minor groove or half-intercalation is the main interaction model between TO-3 dyes and DNA, the introduction of CN into TO-3 dyes would not influence the high selectivity for nucleic acids. **TO3-CN** shows excellent light fastness and large fluorescence Stokes shift (more than 40 nm). Because of its sensitive fluorescence response to nucleic acids with a large

quantum yield (more than 0.7) and low cytotoxicity, this dye may be a potential candidate for nucleic acids detection *in vitro* and nucleus-specific fluorescence imaging *in vivo*.

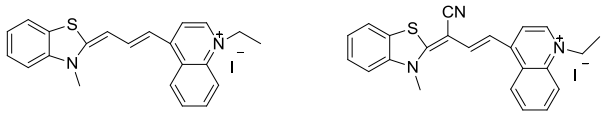

TO3 TO3-CN

Scheme 1. Molecule structure of TO3 and TO3-CN.

Materials and Methods

Materials and Apparatus

All solvents and other chemicals were of reagent grade, and were used without further purification unless otherwise stated. Tris base (tris(hydroxymethyl)aminomethane) was purchased from Promega Co. (USA). SYTO 9 was purchased from Invitrogen (USA). Silica gel (200-300 mesh) and aluminum oxide (neutral. 100-200 mesh) used for flash column chromatography. Calf thymus DNA (ct-DNA) and bovine serum albumin (BSA) were obtained from Sigma Chemical Co. (USA). Saccharomyces cerevisiae RNA (*S. cerevisiae* RNA) was purchased from TaKaRa Biotechnology (Dalian) Co., Ltd. DNase and RNase were purchased from Sigma.

^{1}H NMR and ^{13}C NMR spectra were recorded on a VARIAN INOVA-400 spectrometer with chemical shifts reported as ppm. Mass spectrometric data were obtained on a Q-Tof MS spectrometer (Micromass, Manchester, England). Cell imaging measurements were obtained with spectral confocal microscopes (Olympus, FV1000).

General Methods

All reactions were carried out under a nitrogen atmosphere. Silica gel (200-300 mesh) was used for flash column chromatography. Tris-HCl buffer (pH = 7.4, 10.0 mM,) was prepared using doubly purified water. Stock of ct-DNA is prepared by dissolving commercial nucleic acid in Tris-HCl buffer. The concentration of ct-DNA is determined spectrophotometrically using the molar absorption coefficients of $\varepsilon_{260\ nm}$ = 6600 M^{-1} cm^{-1}. 1 mM stock solutions of **TO3-CN** and **TO3** were prepared in DMSO for the absorption and emission spectral measurements. In the absorption and emission titration studies, the solution of the compound is titrated with aliquots of DNA/RNA stock solution to reach the different mass ratio of DNA/RNA base pairs to the dyes. Concentration of stock solution of BSA was 30 mg mL^{-1}.

Spectroscopic Measurements

Absorption spectra were recorded on an Agilent HP-8453 (Agilent, USA) absorption spectrometer. The steady-state fluorescence emission and excitation spectra were obtained by using a Cray Edipse fluorescence spectrophotometer (Varian, Australia). The fluorescence quantum yields Φ_F^{free}, Φ_F^{DNA}, and Φ_F^{RNA} of dyes were determined according to the literature [29]:

$$\Phi_x = \Phi_s(F_x/F_s)(A_x/A_s)(\lambda_{exs}/\lambda_{exx})(n_x/n_s)^2$$

Where Φ is quantum yield; F is the integrated area under the corrected emission spectrum; A is the absorbance at the excitation wavelength; λ_{ex} is the excitation wavelength; n is the refractive index of the solution; the subscripts x and s refer to the unknown and the standard, respectively. Rhodamine B (Φ_F = 0.97) in methanol was used as the standard [29].

Quantum chemistry calculation

All the quantum-chemical calculations were carried out with the Gaussian 09 suite[30]. The parameters referred to the recent work in our group[31], The ground state structures of dyes were optimized using density functional theory (DFT) with B3LYP functional and 6-31G (d) basis set. The excited state related calculations were carried out with the Time dependent DFT (TD-DFT) based on the optimized structure of the ground state (DFT/6-31G (d)). There are no imaginary frequencies in frequency analysis of all calculated structures; therefore, each calculated structures are in local energy minimum.

Photodegradation experiments

The photodegradation test was carried out in square cross-section quartz cells (l cm × 1 cm) and solutions of the samples were irradiated with a 500 W iodine-tungsten lamp at room temperature. To eliminate the heat and absorb short wavelength light, a cold trap (5 L solution of 60 g/L $NaNO_2$ in 10 cm (width) × 30 cm (length) ×20 cm (height) was set up between the cells and the lamp. The distance between the cells and the lamp was 25 cm. The irreversible bleaching of the dyes at the absorption peak was monitored as a function of time. Samples were tightly sealed, but not deoxygenated with nitrogen before the test.

Cell incubation and imaging

MCF7 (human breast adenocarcinoma cells) and HeLa (human cervical carcinoma cells) cells were cultured in DEME medium supplemented with 10% fetal bovine serum at 37 ℃ in an atmosphere containing 5% CO_2.

For live cell imaging, compounds were added to cells grown in a confocal microscope dish for 45 min and washed with PBS (phosphate-buffered saline) three times. After replacement of the medium, cells were imaged using an OLYMPUS FV1000 confocal fluorescence microscope with a 100×objective lens. For subcellular localization analysis of dyes staining, organelle specific fluorescent dyes were used. MCF7 or HeLa cells were first stained with 2.0 μM of **TO3-CN** at 37 ℃ in an atmosphere of 5% CO_2 for 45min, and then washed with PBS three times. Cells were then incubated with SYTO 9 (3.0 μM) at 37 ℃ in an atmosphere of 5% CO_2 for 45 min, and then washed with PBS three times. After replacement of medium, cells were imaged using an OLYMPUS FV1000 confocal fluorescence microscope with a 100×objective lens.

For DNase and RNase digest test, three sets of pretreated MCF7 cells or HeLa cells were stained with 2 μM **TO3-CN** for 45 min. A total of 100 μL clean PBS (as control experiment), 30 μg/mL DNase (Sigma), or 25 μg/mL DNase-Free RNase (GE) was added into the three adjacent wells and incubated at 37 ℃ in

5% CO_2 for 2 h. Cells were rinsed by clean PBS twice before imaging. For each dyeing test, the fluorescent imaging pictures were obtained with an equal parameter for control. In addition, the DNase and RNase digest test of cells stained with 3 μM SYTO 9 and 3 μM **TO3** were also carried out to make a comparison.

MTT assay for the cell cytotoxicity

Toxicities of **TO3-CN** and **TO3** towards MCF7, HeLa, or cos7 cells were assessed by the standard MTT cytotoxicity assay. This involves the reduction of MTT tetrazolium to MTT formazan pigment by the metabolic activity of living cells. MCF7, HeLa, or cos7 cells were seeded at a density of 1×10^5 cells/mL in a 96-well plate. After 24 h of cell attachment, MCF7, HeLa, or cos7 cells were treated with the three dyes at serial concentrations (0, 1, 3, and 5 μM) for 6 h. Six replicate wells were used for each control and tested concentrations. After incubation for 6 h, the medium was removed and cells were washed with PBS twice. MTT tetrazolium solution (100 μL of 0.5 mg/mL in PBS) was added to each well, and the cells were further incubated at 37 ℃ for 4 h in a 5% CO_2 humidified atmosphere. Excess MTT tetrazolium solution was then carefully removed and the colored formazan was dissolved in 100 μL dimethyl sulfoxide (DMSO). The plate was shaken for 10 minutes and the absorbance was measured at 570 nm and 630 nm using a microplate reader.

Results and discussion

Spectral Properties

The chemical structures of **TO3-CN** (a CN-substituted TO-3) and **TO3** [32] (known compound as the reference) are illustrated in Scheme 1. The spectroscopic properties of the dyes in the absence and presence of DNA or RNA are summarized in Table 1 and Figs. S4–S5. Compared with the control compound **TO3** in aqueous buffer**,** the maximum absorption (543 nm) and emission (611 nm) wavelengths of **TO3-CN** are blue shifted by 83 and 36 nm respectively. However, its maximum emission wavelength is still in the red spectral region. Importantly, the Stokes shift increases substantially from 21 nm (**TO3**) to 67 nm (**TO3-CN**). The optical properties of **TO3-CN** can be attributed to the fact that the electron-withdrawing CN group decreases the electron density of the trimethine chain and thus increases the energy gap for electron excitation, thereby inducing blue shifts in absorption and emission. Additionally, CN group may interrupt the planes of the molecule and thus decreases the rigidity of the molecular structure, thereby increasing the Stokes shift. As shown in Fig. S1, the maximum absorption wavelengths of **TO3-CN** are 543 nm in aqueous solution and 580 nm in dichloromethane, showing an obvious hypsochromic shift in absorption with increased solvent polarity, which is called "negative solvatochromism".[33] Nevertheless, the fluorescence of **TO3-CN** displays no obvious blue shift (Figs. S2 and S3). Moreover, the negative solvatochromism of **TO3-CN** indicates that $S_0\rightarrow S_1$ absorption requires low ground states in a polar environment and a decrease in dipole moment upon electronic excitation.[34] By DFT/TD-DFT, the calculated dipole moment of the ground state for **TO3-CN** is found to be 9.7727, which is higher than that of the excited state (9.5190). By contrast, **TO3** does not exhibit such solvatochromism because the calculated dipole moment of the ground state for **TO3** is 3.9069, which is smaller than that of the excited state (5.0688).

As can be seen from Table 1, after interacting with nucleic acids (CT DNA and RNA) in aqueous solution, **TO3-CN** shows large fluorescence enhancement i.e., the quantum yields are above 0.7 (0.73 for DNA and 0.72 for RNA), which are much higher than those of **TO3** (Φ_F^{DNA} = 0.16 and Φ_F^{RNA} = 0.17). The Stokes shifts of **TO3-CN** are evidently larger (56 nm for DNA and 49 nm for RNA) than those of **TO3** (28 nm for DNA and 20 nm for RNA). The large fluorescence quantum yields and Stokes shift of **TO3-CN** induced by the interaction with nucleic acids are very important for high fluorescence sensitivity and satisfactory image quality.[35]

Table 1. Photophysical data of **TO3** and **TO3-CN**

Compound	λ_{abs} [a](nm)	λ_{em} [b](nm)	Stokes shift (nm)	ε_{max} [c]($M^{-1}cm^{-1}$)	Φ_F [d]	Brightness [e]
TO3 (Buffer[f])	626	647	21	1.5×10^5	0.0019	2.9×10^2
TO3 (DNA)	627	655	28	1.2×10^5	0.16	1.9×10^4
TO3 (RNA)	640	660	20	1.2×10^5	0.17	2.0×10^4
TO3-CN (Buffer)	543	611	68	5.8×10^4	0.017	9.9×10^2
TO3-CN (DNA)	548	604	56	6.2×10^4	0.73	4.5×10^4
TO3-CN (RNA)	565	614	49	5.3×10^4	0.72	3.8×10^4

[a] Absorption maxima. [b] Emission maxima. [c] Molar extinction coefficient. [d] Quantum yield was measured in Tris-HCl buffer (10 mM, pH 7.4), DNA solution or RNA solution. Rhodamine B (Φ_F = 0.97) in methanolic solution was used as a standard. [e] Brightness is defined as the product of the molar extinction coefficient and the quantum yield ($\varepsilon \times \Phi$). [f] Tris-HCl buffer, pH = 7.4, 10 mM.

Photostability of TO3-CN

TO3-CN possesses much better photostability than **TO3.** After 3 h of radiation in aqueous buffer solution, **TO3-CN** remains 90% in optical density, whereas **TO3** remains only less than 20% (Fig. 1a). To examine the imaging performance of the dyes, MCF7 cells were separately incubated with **TO3** (3 μM) and **TO3-CN** (2 μM) at 37 °C for 45 min. Fig. 2b demonstrates that the two dyes are membrane permeable and show clear nucleolar staining as well as faint nucleus and cytoplasm staining under a confocal laser scanning microscope. However, the photobleaching rates in

cells totally differ from each other. In time series, after continuous radiation for 5 min, the fluorescent intensity of **TO3-CN** remains up to 70%, while **TO3** remains below 30% (Figs. 1b, 1c, and 1d). In practical application, the laser scan of microscopy may be set at different time intervals, and highly photostable fluorescent dyes such as **TO3-CN** are urgently needed for the long-term observation of live cells. According to literature, the major photodegradation pathway is the oxidation of cyanine dyes by photogenerated singlet oxygen.[36] Such reaction can be inhibited by the attachment of the cyano group (-CN), which is an electron-accepting group, to partially remove electron density from the trimethine bridge. Thus, the cyano group markedly improves the photostability of **TO3-CN**.[25, 27, 28]

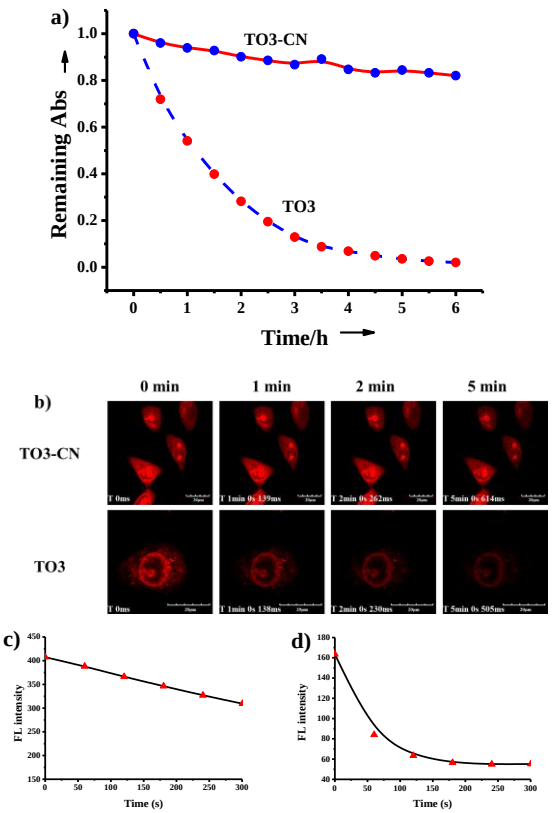

Figure 1 Comparisons of photofading behavior. a) Comparisons of the photofading of **TO3** and **TO3-CN** in Tris-HCl buffer (10 mM, pH 7.4). b) Comparisons of the photofading of **TO3-CN** (2 μM) and **TO3** (3 μM) in MCF 7 cells. c) Fluorescence intensity of **TO3-CN** in MCF7 cells of b). d) Fluorescence intensity of **TO3** in MCF7 cells of b). The scale bar represents 20 μm.

Selectivity to Nucleic Acids of Dyes in Solution and in Cells

TO3-CN also shows high selectivity to nucleic acids over proteins, such as BSA. In **TO3-CN** solution, selective fluorescence enhancements by RNA and DNA are apparent and similar, but BSA represents no such response, similar to **TO3** (Figs. 2a and S6). Deoxyribonuclease (DNase) and ribonuclease (RNase) digest tests were further to prove the DNA/RNA binding. As shown in Fig. 3, the fluorescencec of **TO3-CN** fixed-permeabilized MCF7 cells diminishes with both Dnase and RNase treatments, similar to **TO3** and SYTO 9 which is a widely used green-fluorescent nucleic acid stain[18]. Differently, after Dnase treatment the fluorescence in nucleoli (mainly RNA) and cytoplasm (mainly Ribosomal RNA) remained and after Rnase treatment the fluorescence in nucleoli and cytoplasm greatly decreased, which means **TO3-CN** maintains its good binding affinity to RNA in cells. The similar experimental phenomenon was observed in HeLa (Fig. S9). Based on the shapes of both electronic bands and induced circular dichroism (ICD) bands in the titration of dyes with CT DNA, a great contribution of half-intercalation to the binding modes may be induced (Figs. S7 and S8). The half-intercalation binding modes of dyes and DNA may be the reason of the differenct fluorescence respond to DNA/RNA in cells and in solution.[37] Because in cells the chromatin associated with DNA, histones and non-histone proteins can inhibit elongation and unwinding of the DNA helix, then dye intercalation to the DNA helix in cells becomes more difficult than that in solution. Therefore, **TO3-CN** will ingeneral accumulate in nucleoli and cytoplasmic ribosomes in cells.

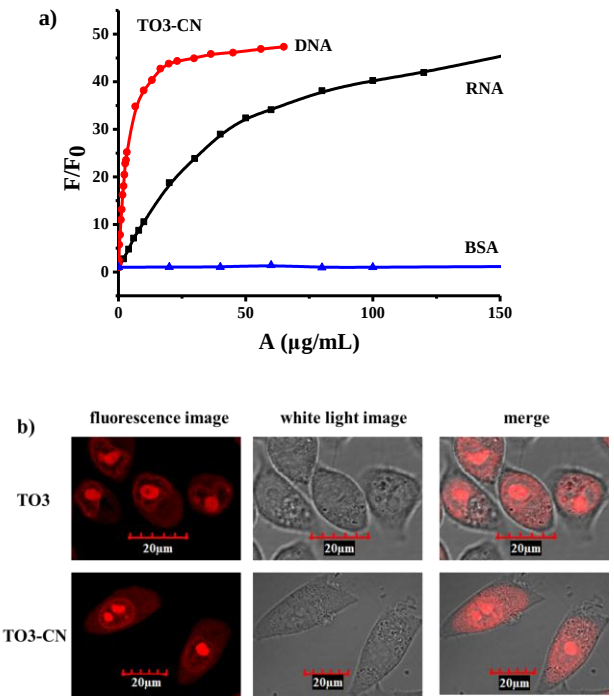

Figure 2 a) Response of selected dyes to DNA, RNA, and BSA in solution. Fluorescence response of **TO3** (1 μM) and **TO3-CN** (1 μM) to CT DNA (red line), tRNA (black line), and BSA (blue line) at different concentrations in Tric-HCl buffer (10 mM, pH 7.4). b) Live-cell staining of dyes in MCF7 cells. **TO3-CN** (excited at 559 nm and collected at 575 nm to 620 nm) was tested at 2 μM concentration for 45 min, and **TO3** (excited at 635 nm and collected at 655 nm to 755 nm) was tested at 3 μM concentration for 45 min. The scale bar represents 20 μm.

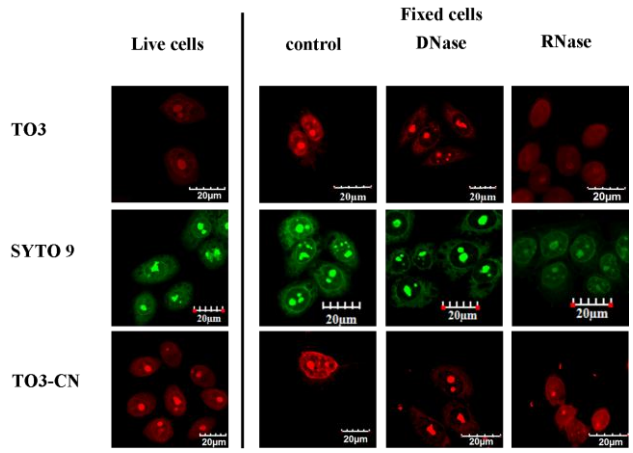

Figure 3 Live-cell staining and DNase and RNase digest experiments with TO3, SYTO 9, and TO3-CN in MCF7. TO3 (excited at 635 nm and collected at 655 nm to 755 nm) and SYTO 9 (excited at 488 nm and collected at 495 nm to 540 nm) were tested at 3 μM concentration for 45 min, and **TO3-CN** (excited at 559 nm and collected at 575 nm to 620 nm) was cultured at 2 μM concentration for 45 min. The scale bar represents 20 μm.

The Subcellular Co-localization of TO3-CN

The subcellular co-localization staining experiments of **TO3-CN** and SYTO 9 were performed in MCF7 cells (Fig. 4) and HeLa cells (Fig. S10). The line scan in Figures 4d and S10d show that the same nuclear regions are labeled with a similar intensity by **TO3-CN** and SYTO 9 in MCF7 and HeLa cells. The same set of images (Figs. 4c and 10c) were used for a colocalization analysis of **TO3-CN** versus SYTO 9, which displayed a high degree of pixel colocalization in MCF7 and HeLa cells. The Pearson's coefficient for MCF7 or HeLa cells are 0.969 and 0.9837, respectively. The results showed that the same localization of **TO3-CN** occurred in different cell lines.

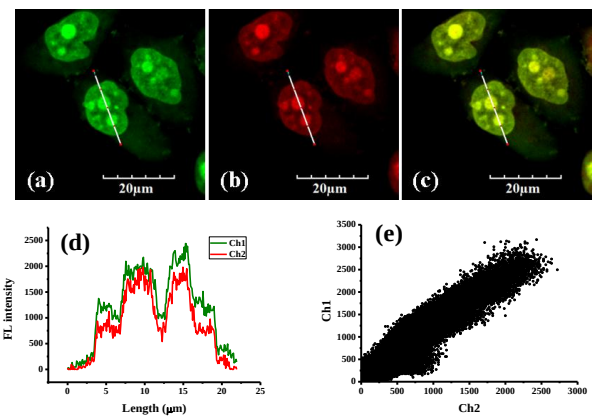

Figure 4 Colocalization imaging of MCF-7 cells stained with 3.0 μM SYTO 9 and 2.0 μM TO3-CN for 45 min at 37 ℃. (a) Confocal image from SYTO 9 on channel 1 (495-535 nm, λ_{ex} = 488 nm). (b) Confocal image from **TO3-CN** on channel 2 (575-620 nm, λ_{ex} = 559 nm). (c) Merged image of channels 1 and 2. (d) Intensity profile of ROIs across MCF-7 cells. (e) Correlation plot of SYTO 9 and **TO3-CN** intensities.

Cytotoxic properties of TO3-CN for Living Cells

The cytotoxicity of **TO3-CN** is low, that is a key feature for living cell imaging.[2, 38] According to a standard MTT assay of MCF7 cells incubation (for 6 h) with 1 or 3 μM **TO3-CN**, the cell viability is more than 80%, similar to **TO3**. At high concentrations, **TO3-CN** is less cytotoxic than **TO3**, such as the case of 5 μM, where the cell viability remains more than 80% for **TO3-CN** but less than 60% for **TO3** (Fig. 5). The standard MTT cytotoxicity assay experiments were also performed with HeLa and cos7 cells (Fig. S11). Both **TO3-CN** and **TO3** show little cytotoxicity (the cell viability is more than 80%) to cos7 cells at all concentrations (1, 3, and 5 μM), while **TO3-CN** shows non-ignorable cytotoxicity to HeLa cells at a relatively high concentration (5 μM). Fortunately, the fact that cytotoxicity of TO3-CN is minimal at working concentration for three cell lines ensures the applicability of this dye as a potentially useful probe for long term imaging nucleic acid in cells.

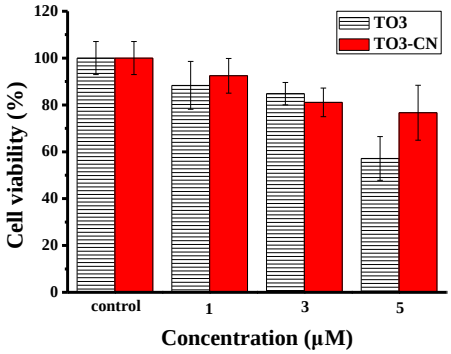

Figure 5 Comparisons of the cytotoxicity of TO3 and TO3-CN at various concentrations (1, 3, and 5 μM) in living MCF7 cells for 6 h.

Conclusion

In conclusion, the introduction of a CN group to the trimethine chain of cyanine dyes can effectively improve photostability and spectral properties. **TO3-CN** is a new dye that has excellent light fastness, large fluorescence Stokes shift, low cytotoxicity, and sensitive fluorescence response with a large quantum yield to nucleic acids. **TO3-CN** may be a potential dye for nucleic acid detection and intracellular fluorescence imaging.

Acknowledgments

This work was financially supported by NSF of China (21136002 and 21376039), National Basic Research Program of China (2013CB733702), Ministry of Education (NCET-12-0080) and NSF of Liaoning (2013020115).

Notes and references

[a] *State Key Laboratory of Fine Chemicals,* [b] *School of Life Science and Biotechnology, Dalian University of Technology, 2 Linggong Road, Hi-tech Zone, Dalian 116024, P.R. China. E-mail:* ***fanjl@dlut.edu.cn****;* ***wangjingyun@dl.cn***

1. M. R. Gill, J. Garcia-Lara, S. J. Foster, C. Smythe, G. Battaglia and J. A. Thomas, *Nature Chemistry*, 2009, **1**, 662-667.

2. Q. Li, Y. Kim, J. Namm, A. Kulkarni, G. R. Rosania, Y. H. Ahn and Y. T. Chang, *Chem. Biol.*, 2006, **13**, 615-623.
3. A. Erve, Y. Saoudi, S. Thirot, C. Guetta-Landras, J. C. Florent, C. H. Nguyen, D. S. Grierson and A. V. Popov, *Nucleic Acids Res.*, 2006, **34**, 1-13.
4. T. P. Constantin, G. L. Silva, K. L. Robertson, T. P. Hamilton, K. Fague, A. S. Waggoner and B. A. Armitage, *Org. Lett.*, 2008, **10**, 1561-1564.
5. S. H. Feng, Y. K. Kim, S. Q. Yang and Y. T. Chang, *Chem. Commun.*, 2010, **46**, 436-438.
6. N. Stevens, N. O'Connor, H. Vishwasrao, D. Samaroo, E. R. Kandel, D. L. Akins, C. M. Drain and N. J. Turro, *J. Am. Chem. Soc.*, 2008, **130**, 7182-7183.
7. M. Chen, Z. Lei, W. Feng, C. Li, Q. M. Wang and F. Li, *Biomaterials*, 2013, **34**, 4284-4295.
8. Z. Li, S. Sun, Z. Yang, S. Zhang, H. Zhang, M. Hu, J. Cao, J. Wang, F. Liu, F. Song, J. Fan and X. Peng, *Biomaterials*, 2013, **34**, 6473-6481.
9. D. R. Pitter, J. Wigenius, A. S. Brown, J. D. Baker, F. Westerlund and J. N. Wilson, *Org Lett*, 2013, **15**, 1330-1333.
10. L. Yuan, W. Lin and H. Chen, *Biomaterials*, 2013, **34**, 9566-9571.
11. J. N. Wilson, J. Wigenius, D. R. Pitter, Y. Qiu, M. Abrahamsson and F. Westerlund, *J Phys Chem B*, 2013, **117**, 12000-12006.
12. S. K. Davis and C. J. Bardeen, *Photochem Photobiol*, 2003, **77**, 675-679.
13. G. P. Pfeifer, Y. H. You and A. Besaratinia, *Mutat Res*, 2005, **571**, 19-31.
14. P. J. Smith, M. Wiltshire, S. Davies, L. H. Patterson and T. Hoy, *J. Immunol. Methods*, 1999, **229**, 131-139.
15. H. P. Easwaran, H. Leonhardt and M. C. Cardoso, *Cell Cycle*, 2005, **4**, 453-455.
16. P. J. Smith, N. Blunt, M. Wiltshire, T. Hoy, P. Teesdale-Spittle, M. R. Craven, J. V. Watson, W. B. Amos, R. J. Errington and L. H. Patterson, *Cytometry*, 2000, **40**, 280-291.
17. K. Wojcik and J. W. Dobrucki, *Cytometry A*, 2008, **73**, 555-562.
18. T. M. P. H. R. P. Haugland, A Guide to Fluorescent Probes and Labeling Technologies, 11th Edition, chap. 8.1. For more detailed information see the website: http://zh.invitrogen.com/site/cn/zh/home/References/Molecular-Probes-The-Handbook/Nucleic-Acid-Detection-and-Genomics-Technology/Nucleic-Acid-Stains.html.
19. X. Peng, F. Song, E. Lu, Y. Wang, W. Zhou, J. Fan and Y. Gao, *J. Am. Chem. Soc.*, 2005, **127**, 4170-4171.
20. P. Li, L. Fang, H. Zhou, W. Zhang, X. Wang, N. Li, H. Zhong and B. Tang, *Chem. Eur. J*, 2011, **17**, 10520-10523.
21. L. Yuan, W. Lin, Y. Xie, B. Chen and J. Song, *Chem. Eur. J*, 2012, **18**, 2700-2706.
22. L. Yuan, W. Lin, Z. Cao, J. Wang and B. Chen, *Chem. Eur. J*, 2012, **18**, 1247-1255.
23. J. R. Johnson, N. Fu, E. Arunkumar, W. M. Leevy, S. T. Gammon, D. Piwnica-Worms and B. D. Smith, *Angew Chem Int Ed Engl*, 2007, **46**, 5528-5531.
24. X. Peng, T. Wu, J. Fan, J. Wang, S. Zhang, F. Song and S. Sun, *Angew Chem Int Ed Engl*, 2011, **50**, 4180-4183.
25. A. Toutchkine, D. V. Nguyen and K. M. Hahn, *Org. Lett.*, 2007, **9**, 2775-2777.
26. B. R. Renikuntla, H. C. Rose, J. Eldo, A. S. Waggoner and B. A. Armitage, *Org. Lett.*, 2004, **6**, 909-912.
27. N. I. Shank, K. J. Zanotti, F. Lanni, P. B. Berget and B. A. Armitage, *J. Am. Chem. Soc.*, 2009, **131**, 12960-12969.
28. N. I. Shank, H. H. Pham, A. S. Waggoner and B. A. Armitage, *J. Am. Chem. Soc.*, 2013, **135**, 242-251.
29. R. A. Velapoldi and H. H. Tonnesen, *J. Fluoresc.*, 2004, **14**, 465-472.
30. M. e. a. G. Frisch, Revision A.02, Gaussian, Inc.,Wallingford CT, 2009.
31. X. J. Peng, Z. G. Yang, J. Y. Wang, J. L. Fan, Y. X. He, F. L. Song, B. S. Wang, S. G. Sun, J. L. Qu, J. Qi and M. Yang, *J. Am. Chem. Soc.*, 2011, **133**, 6626-6635.
32. G. H. K. L. G. S. Brooker, W. W. Williams, *J. Am. Chem. Soc.*, 1942, **64**, 199-210.
33. C. Reichardt, *Chem. Rev.* , 1994, **94**, 2319-2358
34. A. Sytnik and M. Kasha, *Proc. Natl. Acad. Sci. USA*, 1994, **91**, 8627-8630.
35. W. Gao, L. Ji, L. Li, G. Cui, K. Xu, P. Li and B. Tang, *Biomaterials*, 2012, **33**, 3710-3718.
36. M. J. C. T. Dewar, W. , *J. Am. Chem. Soc.*, 1975, **97**, 3978 - 3986.
37. R. W. Horobin, J. C. Stockert and F. Rashid-Doubell, *Histochem Cell Biol*, 2013, **139**, 623-637.
38. L. Xiong, T. Yang, Y. Yang, C. Xu and F. Li, *Biomaterials*, 2010, **31**, 7078-7085.